A negatively charged region of the skeletal muscle ryanodine receptor is involved in Ca^{2+}-dependent regulation of the Ca^{2+} release channel

Salim M. Hayek[a,b], Jiying Zhao[a], Manjunatha Bhat[a], Xuehong Xu[a], Ramakrishnan Nagaraj[a], Zui Pan[a], Hiroshi Takeshima[c], Jianjie Ma[a,*]

[a] *Department of Physiology and Biophysics, Case Western Reserve University School of Medicine, 10900 Euclid Avenue, Cleveland, OH 44106, USA*
[b] *Department of Anesthesiology, Case Western Reserve University School of Medicine, 10900 Euclid Avenue, Cleveland, OH 44106, USA*
[c] *Department of Pharmacology, University of Tokyo Faculty of Medicine, Tokyo 113, Japan*

Received 10 September 1999; received in revised form 21 October 1999

Abstract The ryanodine receptor/Ca^{2+} release channels from skeletal (RyR1) and cardiac (RyR2) muscle cells exhibit different inactivation profiles by cytosolic Ca^{2+}. D3 is one of the divergent regions between RyR1 (amino acids (aa) 1872–1923) and RyR2 (aa 1852–1890) and may contain putative binding site(s) for Ca^{2+}-dependent inactivation of RyR. To test this possibility, we have deleted the D3 region from RyR1 (ΔD3-RyR1), residues 1038–3355 from RyR2 (Δ(1038–3355)-RyR2) and inserted the skeletal D3 into Δ(1038–3355)-RyR2 to generate sD3-RyR2. The channels formed by ΔD3-RyR1 and Δ(1038–3355)-RyR2 are resistant to inactivation by mM $[Ca^{2+}]$, whereas the chimeric sD3-RyR2 channel exhibits significant inactivation at mM $[Ca^{2+}]$. The ΔD3-RyR1 channel retains its sensitivity to activation by caffeine, but is resistant to inactivation by Mg^{2+}. The data suggest that the skeletal D3 region is involved in the Ca^{2+}-dependent regulation of the RyR1 channel.

Key words: Ryanodine receptor; Excitation-contraction coupling; Functional expression; Intracellular calcium release; Lipid bilayer reconstitution; Confocal imaging

1. Introduction

Excitation-contraction (E-C) coupling is the process whereby depolarization of the sarcolemma is translated into myocyte contraction. This signal transduction process occurs at the triad junction, where terminal cisternae of the sarcoplasmic reticulum (SR) abut the transverse tubule of the sarcolemma [1]. The molecular basis of E-C coupling involves the interaction between two proteins, the SR calcium release channel, also referred to as the ryanodine receptor (RyR), and the voltage-gated Ca^{2+} channel of the sarcolemma, also known as the dihydropyridine receptor [2–4]. Three mammalian isoforms of RyR have been identified. RyR1 is mainly found in skeletal muscle [5,6], RyR2 is present in cardiac muscle [7] and RyR3 is referred to as the brain isoform [8]. The three isoforms of RyR are remarkably similar in primary structure, consisting of ~5000 amino acids (aa) with a membrane-spanning domain at the carboxyl-terminal end and a large hydrophilic domain at the amino-terminal end [9]. The carboxyl-terminal domain is predicted to contain 4–12 transmembrane segments, encompassing about one-fifth of the protein size and is thought to form the pore of the Ca^{2+} release channel [10]. The amino-terminus is thought to be cytoplasmic and constitutes the 'foot' region that spans the junctional gap between the SR membrane and the transverse tubule [11].

The isolated Ca^{2+} release channel is regulated by cytoplasmic Ca^{2+} through activation and inactivation mechanisms that are thought to occur at high- and low-affinity Ca^{2+} binding sites on the RyR protein, respectively [12]. In response to Ca^{2+} in the nM to μM concentration range, the Ca^{2+} release channel becomes activated. Higher concentrations of cytoplasmic Ca^{2+} (μM to mM) lead to inactivation of the Ca^{2+} release channel [13,14]. One of the major differences between the skeletal and cardiac RyRs lies in the mechanism of Ca^{2+}-dependent inactivation of the Ca^{2+} release channels. The putative low-affinity binding site for Ca^{2+} has a half dissociation constant that is about 10–20 times larger for cardiac RyR ($K_D \sim 15$ mM) than that for skeletal RyR ($K_D \sim 0.7$ mM) [14]. The molecular basis for this difference is unclear. The primary sequences of RyR1 and RyR2 are relatively well conserved, but differ in three regions referred to as D1, D2 and D3 [15]. The D3 region involves residues 1872–1923 of RyR1 and residues 1852–1890 of RyR2 (Fig. 1A). The D3 region of RyR1 contains a high proportion of negatively charged aa (42 out of 52 total residues are glutamates or aspartates) and has been hypothesized as a possible low-affinity Ca^{2+} binding site [6]. An earlier study from our laboratory showed that a 797 aa deletion mutant of RyR1 involving the D3 region, Δ(1641–2437)-RyR1, displayed altered Ca^{2+}-dependent regulation of the Ca^{2+} release channel expressed in a Chinese hamster ovary (CHO) cell line. Compared with the full-length RyR1 channel, the Δ(1641–2437)-RyR1 was more resistant to inactivation by cytoplasmic Ca^{2+} [16].

To test the role of the D3 region of RyR in the function of the skeletal and cardiac calcium release channels, we generated deletion mutants of RyR1 and RyR2 in which the D3 region was removed. In addition, the aa sequence 1804–1922 encoding the D3 region of RyR1 was introduced into the RyR2 deletion mutant. The functional effects of these mutations were studied by expression of the proteins in CHO cells and lipid bilayer reconstitution of single Ca^{2+} release channels. Our results suggest that the D3 region of RyR1 exerts an important role in Ca^{2+}-dependent regulation of the Ca^{2+} release channel.

2. Materials and methods

2.1. Construction of RyR cDNA mutants

The entire cDNAs for RyR1 and RyR2 were cloned into the eukaryotic expression vectors pRRS11 and pHRRS1, respectively, with transcription occurring under the control of the SV40 promoter [5,17]. Both expression vectors include a neomycin resistance gene, allowing for selection of stable clones. Polymerase chain reaction (PCR)-based

*Corresponding author. Fax: (1) (216) 368-1693.
E-mail: jxm63@po.cwru.edu

PII: S0014-5793(99)01464-7

mutagenesis was utilized to generate a specific deletion of the region encoding D3 (nucleic acids 5616–5769) in pRRS11. PCR products were generated proximal (nucleic acids 4930–5615) and distal (nucleic acids 5770–5950) to D3 [5]. A silent single base mutation at nucleotide 5772 (G to A) was introduced in the PCR primer to generate a unique *Sfu*I restriction site. The two PCR products were subcloned into the pBluescript vector and annealed at the *Sfu*I site. The resulting fragment, lacking the cDNA encoding skeletal D3, was re-introduced into the expression vector pRRS11 to obtain the ΔD3-RyR1 mutant. A deletion mutant of the cardiac RyR lacking aa 1038–3355 was generated by *Xba*I restriction digestion and re-annealing of pHRRS1. The resulting vector is referred to as Δ(1038–3355)-RyR2. Insertion of a PCR product encoding skeletal D3 (nucleic acids 5402–5777, including silent mutations at both ends resulting in *Xba*I sites) into Δ(1038–3355)-RyR2 resulted in sD3-RyR2. In addition, the cDNA encoding ΔD3-RyR1 was subcloned into the mammalian expression vector pCMS-EGFP (Clontech), resulting in pCMS-EGFP-ΔD3-RyR1. pCMS-EGFP is a plasmid that constitutively expresses the enhanced green fluorescent protein (EGFP) as a transfection marker and the protein of interest is driven by a separate cytomegalovirus promoter. A PCR product encoding the D3 region of RyR2 (nucleic acids 5554–5670) was cloned into the *Sfu*I site of pCMS-EGFP-ΔD3-RyR1 to generate cD3-RyR1. All mutant constructs were confirmed by restriction endonuclease digestion and sequencing.

2.2. Cell culture

CHO cells were grown in Ham's F12 medium (Gibco BRL) enriched with 10% fetal bovine serum and supplemented with penicillin (100 U/ml) and streptomycin 100 (μg/ml) in a 5% CO_2 incubator at 37°C. Subculturing was performed using standard techniques. Cells were harvested using a calcium-free phosphate-buffered saline (PBS) solution (containing in mM: NaCl 136.8, KCl 2.68, Na_2HPO_4 8.1, KH_2PO_4 1.47 and EDTA 0.357). Full-length and mutant RyR proteins were expressed in CHO cells using liposome-based methods [10,16]. Transfected CHO cells were exposed to 0.5 mg/ml G418 and selected for stable transfectant clones. Expression of the RyR proteins was determined by Western blotting, measurement of caffeine-induced Ca^{2+} release in single CHO cells and lipid bilayer reconstitution of single Ca^{2+} release channels.

2.3. Immunocytochemistry and Western blot of RyR expression in CHO cells

CHO cells stably expressing RyR were grown on cover slips and fixed in methanol at −20°C for 1 h, using a modified procedure from Takekura et al. [18]. The cells were treated with 5% goat serum in PBS for 1 h to block non-specific antibody binding, followed by incubation with the anti-RyR antibodies [19,20] for 2 h and the cells were then exposed to a Texas red-conjugated secondary antibody for 1 h. The cells were examined on a Carl-Zeiss 410 confocal microscope, using an excitation wavelength of 568 nm and an emission wavelength of 590 nm. Expression of the various RyR mutants in CHO cells was further quantified using Western blot analyses, as described previously [10,16].

2.4. In vivo assay of RyR function

Transfected CHO cells expressing wild-type (wt-) RyR1, ΔD3-

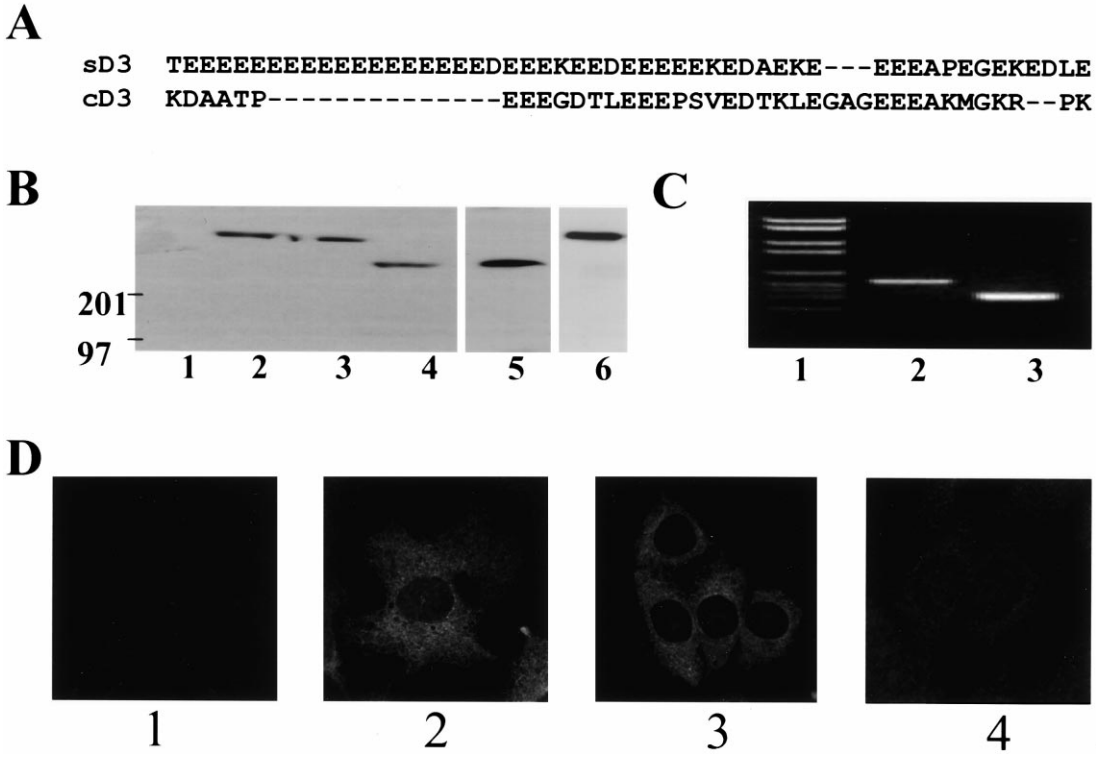

Fig. 1. Expression of RyR proteins in CHO cells. A: Sequence alignment of the D3 region of RyR1 and RyR2. B: Western blot of RyR expressed in CHO cells. Microsomal membrane vesicles from CHO cells expressing wt-RyR1 (lane 2), ΔD3-RyR1 (lane 3), Δ(1038–3355)-RyR2 (lane 4), sD3-RyR2 (lane 5) and cD3-RyR1 (lane 6) were loaded onto a 3–12% linear sodium dodecyl sulfate-polyacrylamide gel. The RyR proteins were probed with a polyclonal antibody (rabbit 46) raised against a conserved 15 aa residues segment of the carboxyl-terminal portion of RyR (aa 5023–5037 of RyR1). Lane 1 was loaded with microsomal membrane vesicles isolated from the untransfected CHO cells. Except for sD3-RyR2, all other RyR constructs were stably expressed in CHO cells. C: PCR analyses of CHO cells expressing wt-RyR1 and ΔD3-RyR1. A 502 bp cDNA fragment was amplified from the genomic DNA of CHO cells expressing wt-RyR1, whereas a PCR product of 346 bp was amplified from CHO cells expressing ΔD3-RyR1. The reduced size reflects the deletion of 156 bp corresponding to the D3 region. D: Immunostaining of untransfected CHO cells (1) and CHO cells stably expressing wt-RyR1 (2), ΔD3-RyR1 (3) and Δ(1038–3355)-RyR2 (4) using Texas red as a conjugate marker. Perinuclear staining consistent with ER distribution of transfected RyR is observed in 100% of the cells but in none of the control untransfected CHO cells. The control CHO cells and those expressing wt-RyR1 and ΔD3-RyR1 were blotted with the monoclonal antibody 34C. The polyclonal rabbit 46 antibody was used to immunoblot Δ(1038–3355)-RyR2, resulting in a weaker signal than 34C.

RyR1, Δ(1038–3355)-RyR2 and sD3-RyR2 were grown in 35 mm dishes and serum-depleted overnight. Cells were then loaded with 2 μM Fura-2-AM for 30 min at 37°C, in a balanced salt solution (containing in mM: NaCl 140, KCl 2.8, $CaCl_2$ 2, $MgCl_2$ 2, glucose 12, HEPES 10 and BSA 0.1%, pH 7.2). Using a dual-wavelength spectrofluorometer, with excitation wavelength of 340 and 380 nm and emission at 510 nm, fluorescence measurements were performed at 37°C in a temperature-regulated chamber, mounted on the stage of an inverted fluorescence microscope (Olympus IX-70). Cells were exposed to 10 mM caffeine (in Ca^{2+}-free solution) by rapid solution exchange. Fura-2 fluorescence signals were continuously monitored at a sampling frequency of 40 Hz and collected using the Felix software (Photon Technology) [21].

2.5. Reconstitution of RyR channels in planar lipid bilayer

A mixture of phosphatidylethanolamine:phosphatidylserine:cholesterol (6:6:1 ratio), dissolved in decane at a concentration of 40 mg/ml, was used to form lipid bilayer membranes across an aperture ~200 μm diameter, separating the *cis* side from the *trans* side. CHO cells stably or transiently expressing the different RyR mutants were harvested and microsomal membrane vesicles were prepared as described previously [16]. Membrane vesicles containing the different RyR mutant channels were added to the *cis* solution and allowed to fuse with the bilayer under a concentration gradient of 200 mM/50 mM Cs-gluconate (*cis*/*trans*). In addition to Cs-gluconate, both *cis* and *trans* solutions included 1 mM $CaCl_2$, 1 mM Cs_2EGTA and 10 mM HEPES (pH 7.4). The free ionic Ca^{2+} concentration was measured using a Ca^{2+}-sensitive electrode (Orion, Model 93-20, Boston, MA, USA) and the values reported are those of free [Ca^{2+}] only. The numbers between parentheses represent the amounts of $CaCl_2$ (in mM) that were added to the *cis* chamber to achieve the following free Ca^{2+} concentrations in mM: 1.0 (5.0), 5.7 (21), 10.0 (33) and 20.1 (57). Channel fusion was facilitated by applying positive voltage and the addition of Ca^{2+} in the *cis* solution to a final free concentration of 220 μM. Channel recordings were performed under symmetrical conditions of 200 mM Cs-gluconate.

2.6. Analysis of single channel data

Single channel data were measured using an Axopatch 200A amplifier patch-clamp unit in combination with a Digidata 1200 A/D-D/A conversion board (Axon Instruments, Foster City, CA, USA) and a Pentium II computer. The bilayer membrane was either held at a particular test potential and channel activity recorded or kept at 0 mV and pulsed to different test potentials, 0.5–1 s in duration. The currents were sampled at 0.2 ms/point and filtered through an eight-pole Bessel filter at 1 kHz. The analysis of single channel data was performed using the pClamp7 program and Sigma plot software. The open probability (P_o) was calculated with respect only to the fully open state of the channel. The total number of experiments was 74 for Δ(1038–3355)-RyR2 ($n = 11$ vesicle preparations), 97 for sD3-RyR2 ($n = 12$ vesicle preparations), 242 for ΔD3-RyR1 ($n = 19$ vesicle preparations) and 16 for cD3-RyR1 ($n = 3$ vesicle preparations).

3. Results

3.1. Expression of RyR in CHO cells

CHO cells were transfected with cDNAs encoding the wt-RyR1, ΔD3-RyR1, Δ(1038–3355)-RyR2, sD3-RyR2 or cD3-RyR1, using liposome-based gene transfection methods. Transiently transfected CHO cells, or single clones of CHO cells that permanently express the different RyR mutants (following selection with G418), were identified by Western blot analysis. As shown in Fig. 1B, the CHO cells stably transfected with wt-RyR1 (lane 2) expressed high molecular weight proteins (~560 kDa), identical to the native RyR from the SR membranes of skeletal muscle. The molecular weights of stably expressed ΔD3-RyR1 (lane 3) and transiently expressed cD3-RyR1 (lane 6) are slightly smaller than that of the wt-RyR1. The stably expressed Δ(1038–3355)-RyR2 (lane 4) and transiently expressed sD3-RyR2 (lane 5) proteins had molecular weights of ~300 kDa and ~320 kDa, as expected for their respective deletions. The stable expression of ΔD3-RyR1 in CHO cells was confirmed by PCR analysis of the genomic DNA (Fig. 1C).

The subcellular localization of wt-RyR1, ΔD3-RyR1 and Δ(1038–3355)-RyR2 stably expressed in CHO cells was examined using immunocytochemistry and confocal microscopy. As shown in Fig. 1D, all three constructs exhibited a perinuclear distribution consistent with the endoplasmic reticulum (ER) membrane localization of the RyR proteins [22].

3.2. In vivo and in vitro assays of RyR expressed in CHO cells

We have shown previously that the cells expressing either wt-RyR1 or wt-RyR2 can release intracellular Ca^{2+} in response to stimulation with caffeine [22,23]. To assay the in vivo function of these RyR mutants, transfected CHO cells were loaded with Fura-2 and Ca^{2+} release from the ER was measured in single CHO cells in response to stimulation with 10 mM caffeine. As shown in Fig. 2A, caffeine triggered rapid release of Ca^{2+} from the ER membrane in cells expressing wt-RyR1, ΔD3-RyR1 and cD3-RyR1 but there was no response in cells expressing Δ(1038–3355)-RyR2 or sD3-RyR2. The lack of caffeine-induced Ca^{2+} release is not due to depletion of Ca^{2+} from the ER, since application of ATP (0.1 mM) led to rapid intracellular Ca^{2+} release in all transfected cells, including Δ(1038–3355)-RyR2 and sD3-RyR2. ATP binds to purinergic receptors at the cell membrane leading to generation of IP3 and subsequent activation of the IP3 receptor [24]. Thus, deletion of D3 from RyR1 maintains the caffeine-dependent activation of the RyR1 channel, but a larger deletion of the cytoplasmic domain of RyR2 (aa 1038–3355) eliminates the caffeine-dependent activation of RyR2.

To study the functional activity of single RyR channels, microsomal membrane vesicles were prepared from CHO cells expressing the various RyR proteins. Fusion of these vesicles with the lipid bilayer resulted in incorporation of functional Ca^{2+} release channels. To facilitate identification of the Ca^{2+} release channels, we used Cs-gluconate as the current-carrying ion in the recording solution. The use of Cs as current carrier allows for buffering of the free [Ca^{2+}] to any desired level. In addition, Cs eliminates most of the potassium channel activities present in the microsomal membrane vesicles and the large anion gluconate does not permeate through the endogenous chloride channels present in the ER membranes of CHO cells. All mutant RyR proteins formed functional channels with fast transitions between conductance states in symmetric 200 mM Cs-gluconate (Fig. 2). Opening of these channels required the presence of μM concentrations of cytosolic Ca^{2+} and application of ryanodine (5–40 μM) resulted in the appearance of long subconductance states, characteristic of a ryanodine effect on the Ca^{2+} release channels (not shown).

3.3. Ca^{2+}-dependent regulation of wt-RyR1 and ΔD3-RyR1 channels

Similar to the wt-RyR1 channel, the ΔD3-RyR1 channel exhibits fast transitions between open and closed states in 200 mM Cs-gluconate. Opening of both wt-RyR1 and ΔD3-RyR1 channels requires the presence of μM [Ca^{2+}] in the cytosolic solution, as chelation of the free Ca^{2+} to nM concentrations results in complete closure of both channels (Fig. 3A). A striking difference between the ΔD3-RyR1 and wt-RyR1 channels is observed, however, when the cytoplasmic [Ca^{2+}] is increased to mM concentrations. The wt-RyR1 chan-

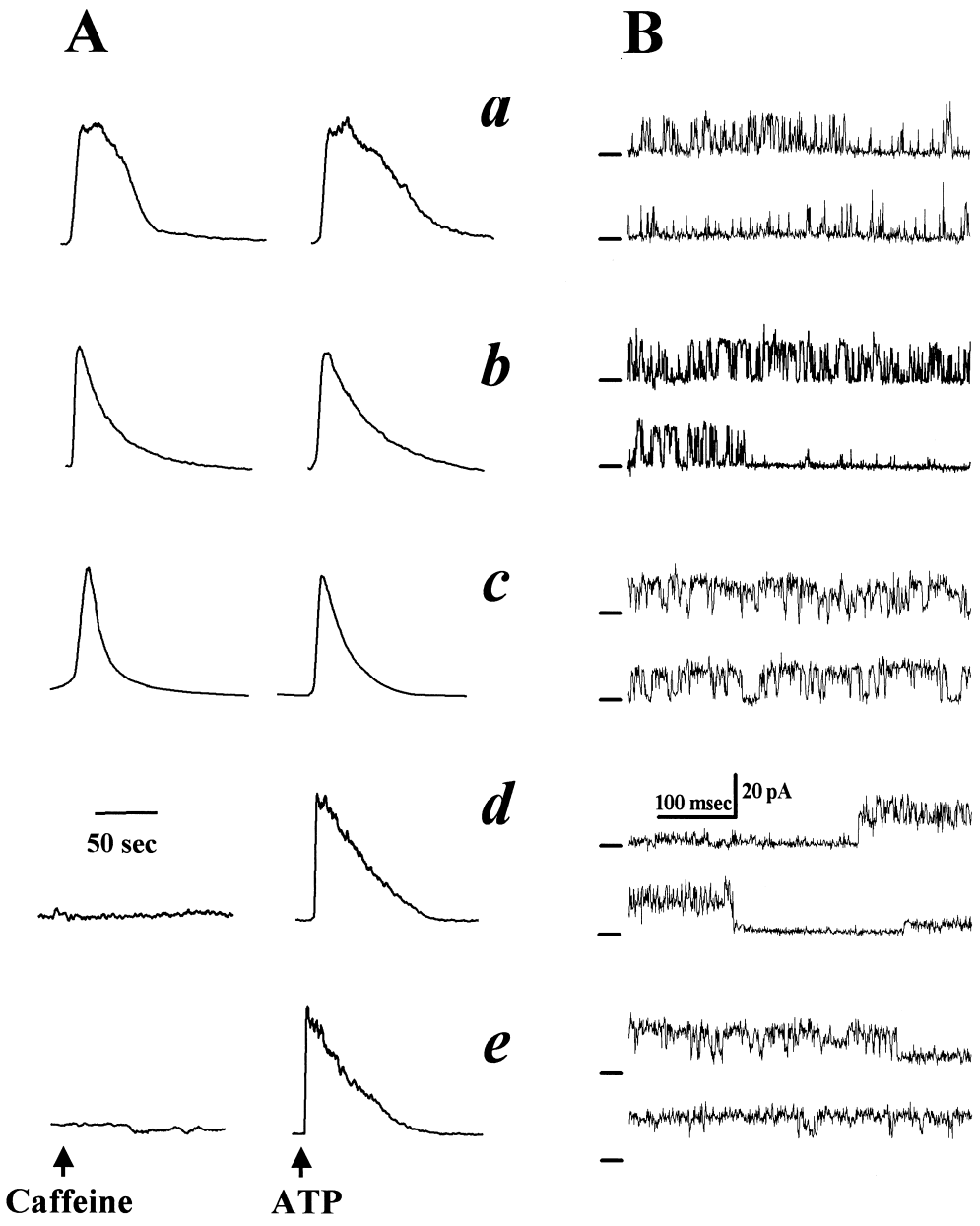

Fig. 2. Caffeine-induced Ca^{2+} release and single channel recordings of RyR expressed in CHO cells. A: Caffeine-induced Ca^{2+} release from CHO cells expressing RyR proteins. The recorded increases in intracellular Ca^{2+} (measured with the 340/380 fluorescence ratio of Fura-2) were acquired from single CHO cells following stimulation with 10 mM caffeine, in the absence of extracellular Ca^{2+}. Cells expressing wt-RyR1 (a), ΔD3-RyR1 (b) and cD3-RyR1 (e) exhibit rapid Ca^{2+} release in response to caffeine, whereas those stably expressing Δ(1038–3355)-RyR2 (d) and those transiently expressing sD3-RyR2 (e) do not support caffeine-induced Ca^{2+} release. All cell types maintain intact ER Ca^{2+} pools, as revealed by the similar responses to ATP-induced Ca^{2+} release. The traces are representatives of over six other cells tested for each preparation. B: Representative single channel currents through the different RyR mutants were recorded at +50 mV test potential with 200 mM symmetric Cs-gluconate as the current carrier, in the presence of 220 μM Ca^{2+} in the cytosolic solution.

nel displays near complete inactivation at $[Ca^{2+}] \sim 5.7$ mM, but in contrast, the open probability (P_o) of the ΔD3-RyR1 channel does not appear to decrease when the cytosolic $[Ca^{2+}]$ is increased as high as 20 mM (Fig. 3A). To analyze the P_o as a function of $[Ca^{2+}]$, the cytoplasmic $[Ca^{2+}]$ was changed by adding $CaCl_2$ or EGTA and the Ca^{2+} inactivation and activation curves were respectively obtained. Compared to wt-RyR1, the Ca^{2+} inactivation curve for ΔD3-RyR1 is markedly shifted to the right. The peak P_o for ΔD3-RyR1 is observed at 2.31 mM Ca^{2+} (0.237 ± 0.074). In contrast, the wt-RyR1 P_o is maximal (0.187 ± 0.032) at 220 μM Ca^{2+} and decreases steadily afterwards (Fig. 3C). At $[Ca^{2+}] = 20.1$ mM, the P_o of ΔD3-RyR1 (0.138 ± 0.019) is similar to that obtained at 220 μM Ca^{2+} (0.136 ± 0.017), whereas the wt-RyR1 channel is all but completely closed ($P_o = 0.001 \pm 0.001$). These results are similar to our previous study with Δ(1641–2437)-RyR1 [16]. Of note, wt-RyR1 displays a higher P_o at 1 mM Ca^{2+} compared to native RyR1 [14]. This may be related to the absence of muscle-specific accessory proteins in the CHO cells [16].

Interestingly, the Ca^{2+} activation curve of the ΔD3-RyR1 channel is shifted to the left, compared to wt-RyR1, reflecting an increased sensitivity of the Ca^{2+} release channel to nM

[Ca^{2+}] (Fig. 3B). This contrasts with the rightward shift of the activation curve of Δ(1641–2437)-RyR1 [16]. Although we do not know the exact reason for this discrepancy, it probably stems from a different conformational change imparted by a deletion of 797 residues of the amino-terminal domain of RyR1 (Δ(1641–2437)-RyR1) vs. a deletion of only 52 residues (ΔD3-RyR1). Similar to Δ(1641–2437)-RyR1 [16], the ΔD3-RyR1 channel exhibits inward rectification at positive voltages (not shown). Thus, in our recordings (+50 mV), the unitary currents through ΔD3-RyR1 channels are about 20% smaller than those recorded through wt-RyR1.

3.4. Ca^{2+}-dependent regulation of Δ(1038–3355)-RyR2 and sD3-RyR2 channels

In preliminary studies with the full-length RyR2 expressed in CHO cells, we observed a dose-dependent, and complete, inactivation of the wt-RyR2 channel by cytosolic Ca^{2+}. Compared with the wt-RyR1 channel, the Ca^{2+}-dependent inactivation of the wt-RyR2 channel was shifted to the right. But the difference between the recombinant wt-RyR1 and wt-RyR2 channels was significantly less than that observed with the native Ca^{2+} release channels from skeletal and cardiac muscles [14]. This likely reflects the role of accessory proteins in the overall function of the Ca^{2+} release channels. To study the potential role of the D3 region in the inactivation property of the Ca^{2+} release channel, a clear phenotype was needed, one that does not inactivate in response to high [Ca^{2+}]. Based on our experience with skeletal RyR-C [10], a large 'foot' region deletion was undertaken in RyR2 (Δ(1038–3355)-RyR2), with the aim of obtaining a functional channel that does not inactivate in response to high [Ca^{2+}]. sD3-RyR2 was generated to study the role of skeletal D3 in the Ca^{2+}-dependent regulation of RyR.

Despite deletion of a large portion of the cytosolic domain of RyR2, both Δ(1038–3355)-RyR2 and sD3-RyR2 channels still retain the Ca^{2+} activation characteristic of RyR and are sensitive to modulation by ryanodine (not shown). However, compared with the wt-RyR2 channel, the open probabilities of Δ(1038–3355)-RyR2 and sD3-RyR2 channels are significantly higher and the mutant channels exhibit altered conductance patterns [23]. At 220 μM Ca^{2+}, the average P_o for wt-RyR2 was 0.215 ± 0.035, 0.542 ± 0.102 for Δ(1038–3355)-RyR2 and 0.543 ± 0.052 for sD3-RyR2. To compare the Ca^{2+}-dependent inactivation of the Δ(1038–3355)-RyR2 and sD3-RyR2 channels, the cytosolic [Ca^{2+}] was increased from μM up to mM concentrations. As shown in Fig. 4A, the Δ(1038–3355)-RyR2 channel does not display apparent inactivation at mM [Ca^{2+}]. In contrast, the sD3-RyR2 channel does exhibit significant inactivation under similar conditions of elevated *cis* [Ca^{2+}] (Fig. 4B). Thus, deletion of aa 1038–3355 from RyR2 completely eliminates Ca^{2+}-dependent inactivation of the RyR2 channel and insertion of skeletal D3 into the cardiac deletion mutant Δ(1038–3355)-RyR2 restores Ca^{2+}-dependent inactivation of the Ca^{2+} release channel. Without a clear phenotypic difference between the wt-RyR1 and wt-RyR2 channels, we did not pursue functional comparisons between the wt-RyR2 and chimeric cardiac D3 in RyR1.

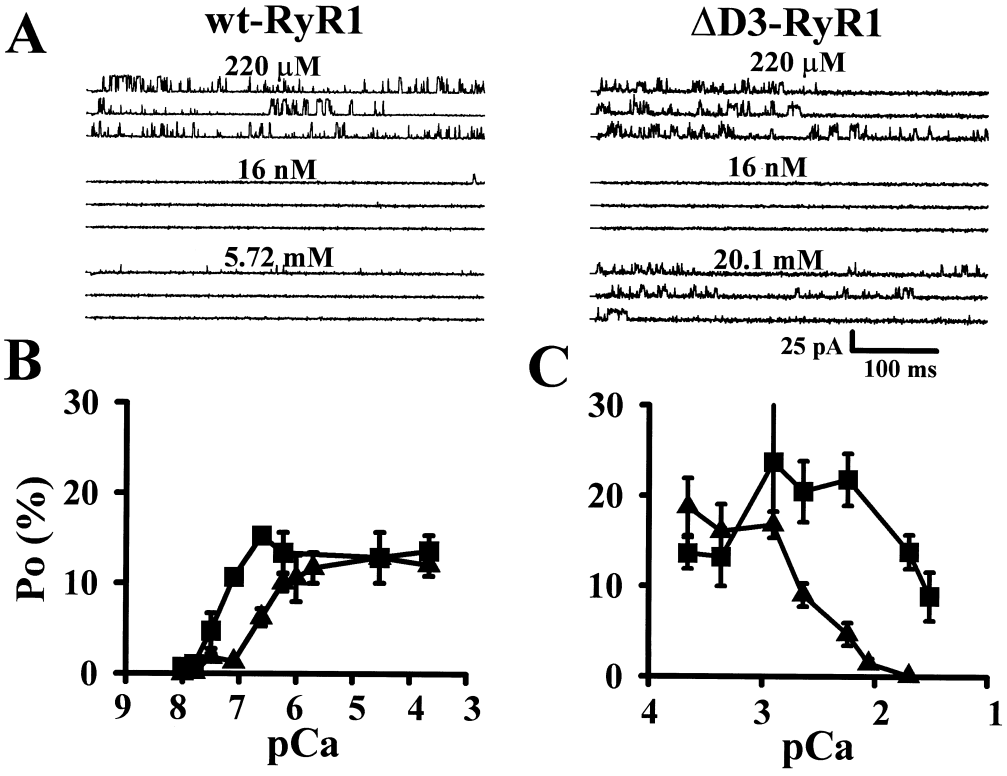

Fig. 3. Ca^{2+}-dependent regulation of wt-RyR1 and ΔD3-RyR1. Representative single channel currents from wt-RyR1 and ΔD3-RyR1 at 220 μM (upper panels), 16 nM (middle panels) and elevated [Ca^{2+}] (bottom panels) (A). While both channel types displayed preserved Ca^{2+} activation properties (middle panels), the ΔD3-RyR1 channel exhibited marked resistance to inactivation by mM [Ca^{2+}] (bottom panels). Open probabilities (P_o) of the wt-RyR1 (▲) and ΔD3-RyR1 (■) channels were plotted as a function of the cytosolic [Ca^{2+}]. Each data point represents the mean ± S.E.M. ($n = 6$–30). Compared with the wt-RyR1 channel, the activation curve of the ΔD3-RyR1 channel was shifted to the left (B) and inactivation was shifted to the right (C).

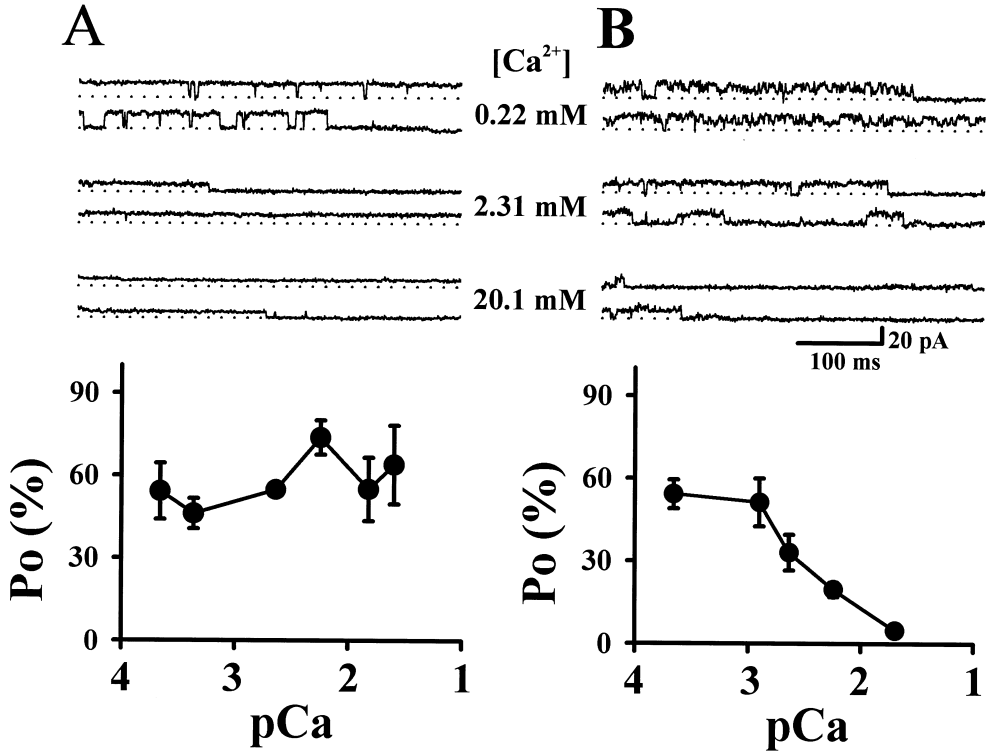

Fig. 4. Ca^{2+}-dependent inactivation of the Δ(1038–3355)RyR2 and sD3-RyR2. Selected single channel currents from Δ(1038–3355)-RyR2 (A) and sD3-RyR2 (B) were obtained under the same recording conditions as shown in Fig. 2B. Increasing the cytosolic $[Ca^{2+}]$ to 20.1 mM leads to significant inactivation of the sD3-RyR2 channels, but no change in activity of the Δ(1038–3355)-RyR2 channel. The open probabilities of the Δ(1038–3355)-RyR2 and sD3-RyR2 channels were calculated at +50 mV test potential, with cytosolic $[Ca^{2+}]$ ranging from 220 μM to 20.1 mM. Each data point represents the average over 4–12 different experiments.

3.5. Effect of Mg^{2+} on the wt-RyR1 and ΔD3-RyR1 channels

To further test the function of the D3 region of RyR1 as a potential low-affinity Ca^{2+} inactivation site(s), we compared the effect of Mg^{2+} on the wt-RyR1 and ΔD3-RyR1 channels. As shown in Fig. 5A, application of 30 mM $MgCl_2$ to the cytosolic solution resulted in complete closure of the wt-RyR1 channel, but no inhibitory effect on the ΔD3-RyR1 channel was observed even after addition of 60 mM $MgCl_2$. A decrease in the P_o and to a lesser extent of single channel conductance is noted with wt-RyR1 but not with ΔD3-RyR1. The lack of an effect of Mg^{2+} on the ΔD3-RyR1 channel (both P_o and conductance) may reflect the altered binding affinity of the mutant channel to Mg^{2+} or the altered permeation properties of the channel to Mg^{2+}.

The data shown in Fig. 5B demonstrate that the ΔD3-RyR1 channel is resistant to inhibition by Mg^{2+}. This is consistent

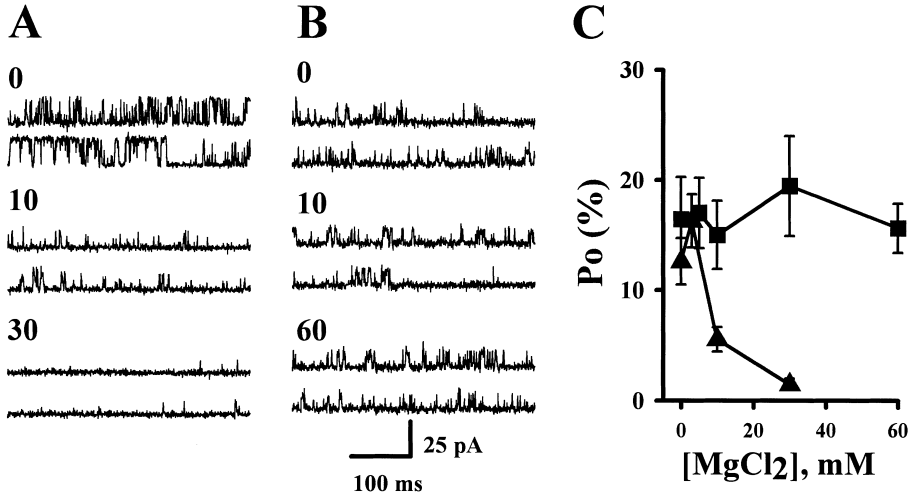

Fig. 5. Effects of Mg^{2+} on the wt-RyR1 and ΔD3-RyR1 channels. The current traces from a wt-RyR1 channel (A) or a ΔD3-RyR1 channel (B) were acquired at $[Ca^{2+}] = 220$ μM in 200 mM Cs-gluconate, at a test potential of +50 mV, in the presence of different concentrations of $MgCl_2$. Open probabilities (P_o) of wt-RyR1 (▲) and ΔD3-RyR1 (■) were plotted as a function of $[MgCl_2]$ added to the *cis* solution (C). $n = 9$ for ΔD3-RyR1 and $n = 4$ for wt-RyR1.

with observations from other investigators, suggesting that Mg^{2+} inhibits the skeletal muscle Ca^{2+} release channel via interaction with a putative Ca^{2+} inactivation domain on the RyR1 protein [12,25].

4. Discussion

Ca^{2+}-dependent inactivation of the RyR channels plays an important role in E-C coupling in cardiac and skeletal muscle cells, acting as an alternative mechanism to terminate the Ca^{2+} release process following an action potential stimulation [26,27]. It is well known that the skeletal and cardiac Ca^{2+} release channels respond differently to inactivation by cytosolic Ca^{2+} and regions of divergence between the primary sequences of RyR1 and RyR2 have been proposed as possible explanatory mechanisms [16]. In this study, we show that deletion of the D3 region from RyR1 results in functional Ca^{2+} release channels that are more sensitive to activation by low cytosolic [Ca^{2+}] and markedly resistant to inactivation by elevated cytoplasmic [Ca^{2+}]. This may reflect loss of a Ca^{2+} inactivation binding site or change in the conformation of the Ca^{2+} release channel, resulting in resistance to modulation by elevated cytosolic [Ca^{2+}]. The fact that a chimeric mutant of RyR2, sD3-RyR2, consisting of skeletal D3 inserted into Δ(1038–3355)-RyR2, exhibits significant Ca^{2+}-dependent inactivation argues strongly in favor of an active role of the D3 region of RyR1 in the Ca^{2+} inactivation process.

Ca^{2+}-dependent activation and inactivation of RyR occur at spatially distinct binding sites, since mutant constructs of RyR1 and RyR2 lacking D3 displayed resistance to inactivation by Ca^{2+}, but retained Ca^{2+} activation properties. The cytoplasmic domain of RyR2 appears to be important for the function of the Ca^{2+} release channel, as deletion of aa 1038–3355 from RyR2 affected not only the Ca^{2+}-dependent inactivation of the RyR2 channel but also the response to caffeine. This is consistent with our earlier observations with the RyR-C channel lacking aa 183–4006 of RyR1. This truncated channel maintains Ca^{2+}-dependent activation but lacks Ca^{2+}-dependent inactivation and caffeine-induced Ca^{2+} release [10,22]. Furthermore, the open probabilities of the Δ(1038–3355)-RyR2 and sD3-RyR2 channels are significantly higher than those of the wt-RyR2 and wt-RyR1 channels, at μM to low mM [Ca^{2+}]. Both deletion channels exhibit conductance changes even though the deleted segments (1872–1923 of RyR1 and 1038–3355 of RyR2) in the primary sequence lie distant from the putative pore [28]. This indicates that domains in the 'foot' region of RyR may interact with the carboxyl-terminal/pore region and affect channel function or alternatively, deletion of these segments could introduce allosteric changes in the protein structure and affect the overall permeation and regulatory properties of the Ca^{2+} release channel. These results, when taken together, reflect the importance of regulatory domains of the 'foot' region of RyR in modulating the Ca^{2+} release channel activity.

The inhibition of RyR by Mg^{2+} has been proposed to involve two independent processes [12,25]. Mg^{2+} may inhibit the RyR channel by competing with Ca^{2+} (type I inhibition) at the high-affinity Ca^{2+} binding site. Alternatively, Mg^{2+} may bind to the low-affinity Ca^{2+} binding site, which does not discriminate between Ca^{2+} and Mg^{2+}, and inactivate the Ca^{2+} release channel (type II inhibition). The resistance to inactivation by Mg^{2+} of the ΔD3-RyR1 channel, at 220 μM Ca^{2+}, suggests that Mg^{2+} ions interact with the D3 region of RyR1 to effect inactivation of the Ca^{2+} release channel (type II inhibition). Taken together, our data indicate that the skeletal D3 region likely represents a putative Ca^{2+} regulatory domain of the RyR1 channel that is involved in Ca^{2+}- and Mg^{2+}-dependent inactivation of the Ca^{2+} release channel.

Du and MacLennan used a [^{3}H]ryanodine binding assay with chimeric constructs between RyR1 and RyR2 and concluded that the Ca^{2+} inactivation sites are located in the carboxyl-terminal quarter of the RyR1 protein [29]. In their studies with the detergent-solubilized RyR proteins, the full-length RyR2 did not show apparent Ca^{2+}-dependent inactivation at [Ca^{2+}] as high as 20 mM. But studies from other investigators and our laboratory (unpublished data with the wt-RyR2 expressed in CHO cells) have shown that RyR2 does display inactivation at elevated mM [Ca^{2+}] [14]. Thus, while the [^{3}H]ryanodine binding approach using solubilized chimeric constructs of RyR1 and RyR2 may help to address the functional difference between the two proteins, a better understanding of the fundamental mechanism for Ca^{2+}-dependent regulation of the Ca^{2+} release channels requires further structure-function studies. It is possible that multiple interacting Ca^{2+} binding sites reside on the RyR proteins (some on the foot region, e.g. D3 region, and some on the carboxyl-terminal end) and participate in the overall regulation of the Ca^{2+} release channel function.

In addition to its role in the Ca^{2+}-dependent regulation of the Ca^{2+} release channel, the D3 region of RyR1 may play an important role in the E-C coupling process. The molecular determinants of the E-C coupling in skeletal muscle involve the II-III loop of the dihydropyridine receptor and as yet an undetermined component in the 'foot' region of RyR1. Cytoplasmic regions that are divergent between RyR1 and RyR2 (i.e. D2 or D3) appear to be the most likely candidates to interact with DHPR. Using dyspedic myotubes that lack endogenous RyR1 and RyR3, Yamazawa et al. [30] demonstrated that expression of a mutant RyR1 channel lacking residues 1303–1406 (includes D2) abolished skeletal type E-C coupling. However, this region alone does not determine the functional difference in E-C coupling between skeletal and cardiac muscles, since a chimeric construct containing the corresponding region (D2) of RyR2 is capable of restoring skeletal type E-C coupling. A separate study by Nakai et al. [31] reported that a chimeric construct consisting of residues 1635–2636 of RyR1 (includes D3) inserted into RyR2, mediated skeletal type E-C coupling in dyspedic myotubes and enhanced the Ca^{2+} channel function of DHPR. Future studies with D3 mutants expressed in dyspedic myotubes should provide further insights into the role of the D3 region in the E-C coupling process of skeletal and cardiac muscle cells.

Acknowledgements: We are grateful to Dr K.P. Campbell for generous supply with the polyclonal antibodies against RyR. We also thank Dr D. Damron for assistance with the Ca^{2+} release experiments. This work was supported by NIH Grant RO1-AG15553 and an established investigatorship from the American Heart Association to J. Ma and a postdoctoral fellowship from the American Heart Association (Ohio Affiliate) to M.B. Bhat.

References

[1] Franzini-Armstrong, C. and Protasi, F. (1997) Physiol. Rev. 77, 699–729.
[2] Catterall, W.A. (1991) Cell 64, 871–874.

[3] Somlyo, A.P. and Somlyo, A.V. (1994) Alcohol Clin. Exp. Res. 18, 138–143.
[4] Meissner, G. (1994) Annu. Rev. Physiol. 56, 485–508.
[5] Takeshima, H., Nishimura, S., Matsumoto, T., Ishida, H., Kangawa, K., Minamino, N., Matsuo, H., Ueda, M., Hanaoka, M., Hirose, T. and Numa, S. (1989) Nature 339, 439–445.
[6] Zorzato, F., Fujii, J., Otsu, K., Phillips, M., Green, N.M., Lai, F.A., Meissner, G. and MacLennan, D.H. (1990) J. Biol. Chem. 265, 2244–2256.
[7] Otsu, K., Willard, H.F., Khanna, V.K., Zorzato, F., Green, N.M. and MacLennan, D.H. (1990) J. Biol. Chem. 265, 13472–13483.
[8] Hakamata, Y., Nakai, J., Takeshima, H. and Imoto, K. (1992) FEBS Lett. 312, 229–235.
[9] Takeshima, H. (1993) Ann. N.Y. Acad. Sci. 707, 165–177.
[10] Bhat, M.B., Zhao, J., Takeshima, H. and Ma, J. (1997) Biophys. J. 73, 1329–1336.
[11] Wagenknecht, T. and Radermacher, M. (1997) Curr. Opin. Struct. Biol. 7, 258–265.
[12] Meissner, G., Darling, E. and Eveleth, J. (1986) Biochemistry 25, 236–244.
[13] Ma, J., Fill, M., Knudson, C.M., Campbell, K.P. and Coronado, R. (1988) Science 242, 99–102.
[14] Laver, D.R., Roden, L.D., Ahern, G.P., Eager, K.R., Junankar, P.R. and Dulhunty, A.F. (1995) J. Membr. Biol. 147, 7–22.
[15] Sorrentino, V. and Volpe, P. (1993) Trends Pharmacol. Sci. 14, 98–103.
[16] Bhat, M.B., Zhao, J., Hayek, S., Freeman, E.C., Takeshima, H. and Ma, J. (1997) Biophys. J. 73, 1320–1328.
[17] Nakai, J., Imagawa, T., Hakamat, Y., Shigekawa, M., Takeshima, H. and Numa, S. (1990) FEBS Lett. 271, 169–177.
[18] Takekura, H., Takeshima, H., Nishimura, S., Takahashi, M., Tanabe, T., Flockerzi, V., Hofmann, F. and Franzini Armstrong, C. (1995) J. Muscle Res. Cell Motil. 16, 465–480.
[19] Airey, J.A., Beck, C.F., Murakami, K., Tanksley, S.J., Deerinck, T.J., Ellisman, M.H. and Sutko, J.L. (1990) J. Biol. Chem. 265, 14187–14194.
[20] McPherson, P.S., Kim, Y.K., Valdivia, H., Knudson, C.M., Takekura, H., Franzini-Armstrong, C., Coronado, R. and Campbell, K.P. (1991) Neuron 7, 17–25.
[21] Hamada, H., Damron, D.S., Hong, S.J., Van, W.D. and Murray, P.A. (1997) Circ. Res. 81, 812–823.
[22] Bhat, M.B., Zhao, J., Zang, W., Balke, C.W., Takeshima, H., Wier, W.G. and Ma, J. (1997) J. Gen. Physiol. 110, 749–762.
[23] Bhat, M.B., Hayek, S., Zhao, J., Zang, W., Takeshima, H., Wier, W.G. and Ma, J. (1999) Biophys. J. 77, 808–816.
[24] Putney, J.W. (1997) Cell Calcium 21, 257–261.
[25] Laver, D.R., Baynes, T.M. and Dulhunty, A.F. (1997) J. Membr. Biol. 156, 213–229.
[26] Valdivia, H.H., Kaplan, J.H., Ellis Davies, G.C. and Lederer, W.J. (1995) Science 267, 1997–2000.
[27] Fabiato, A. (1985) J. Gen. Physiol. 85, 247–289.
[28] Zhao, M., Li, P., Li, X., Zhang, L., Winkfein, R.J. and Chen, S.R. (1999) J. Biol. Chem. 274, 25971–25974.
[29] Du, G.G. and MacLennan, D.H. (1999) J. Biol. Chem. 274, 26120–26126.
[30] Yamazawa, T., Takeshima, H., Shimuta, M. and Iino, M. (1997) J. Biol. Chem. 272, 8161–8164.
[31] Nakai, J., Sekiguchi, N., Rando, T.A., Allen, P.D. and Beam, K.G. (1998) J. Biol. Chem. 273, 13403–13406.